Proceedings of the IASS Annual Symposium 2016
"Spatial Structures in the 21st Century"
26-30 September, 2016, Tokyo, Japan
K. Kawaguchi, M. Ohsaki, T. Takeuchi (eds.)

Zero-Area Reciprocal Diagram of Origami

Erik D. DEMAINE[a], Martin L. DEMAINE[a], David A. HUFFMAN[b],
Thomas C. HULL[c], Duks KOSCHITZ[d], Tomohiro TACHI*

* The University of Tokyo
3-8-1 Komaba, Meguro-Ku, Tokyo 153-8902, Japan
tachi@idea.c.u-tokyo.ac.jp
[a] Massachusetts Institute of Technology
[b] University of California, Santa Cruz
[c] Western New England University
[d] Pratt Institute

Abstract

We propose zero-area reciprocal diagram as a graphical tool for the design of rigid foldable mechanisms. First, we interpret the meaning of zero-area reciprocal diagram as the second-order approximation of rigid foldability of origami crease pattern. We further show the equivalence to rigid foldability for special cases of single-vertex origami and an origami pattern with flat foldable degree-4 vertices. We also show design examples with approximated rigid folding.

Keywords: morphology, origami, reciprocal diagram, first-order flexibility, second-order flexibility

1. Introduction

The reciprocal diagram is a powerful graphical tool for understanding and designing structural systems. If we give a truss structure as an original form diagram, its reciprocal diagram represents a force diagram representing the equilibrium. If we give a crease pattern as an original form diagram, then its reciprocal diagram represents its polyhedral lifting, which is a polyhedral surface whose planar projection is precisely the original diagram [3, 12]. These two interpretations are related: the polyhedral lifting represents the Airy stress function of the truss under stress [7], where the fold angle (measured by tangents) of the polyhedral edge is equivalent to the force applied to each edge.

In the context of origami, we can view a polyhedral lifting as the first-order approximation of *rigid origami*, i.e., an origami surface is composed of rigid panels and rotational hinges connecting them together. Hence, it seems proper to use the reciprocal diagram for the analysis of *rigid foldability* and the design of *rigidly foldable* structures. However, it turns out soon that the existence of reciprocal diagram alone is a poor tool to judge rigid foldability of origami. For example, a degree-3 vertex has a nontrivial reciprocal diagram, but there is no valid folding for this pattern (Figure 1).

David Huffman, the third author of this paper, introduced the concept of *dual picture* in 1970s [5] for analyzing polyhedral surface with zero Gaussian curvature, i.e., paper folding. In this paper, we call a dual picture a *zero-area reciprocal diagram* as it is a reciprocal diagram with an additional property that the signed area of each face is zero. Figure 2 shows an example of origami vertex and its zero-area reciprocal diagram. Huffman designed series of origami patterns in 1970's, when he apparently used the zero-area reciprocal diagram in his design sketch. However, the precise meaning of the diagram

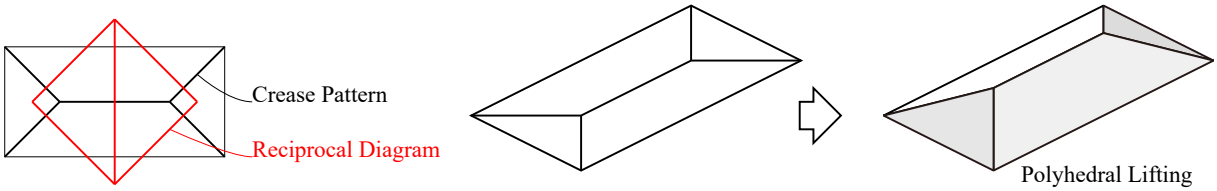

Figure 1: A pattern with degree-3 vertices has a nontrivial reciprocal diagram, but is not finitely foldable.

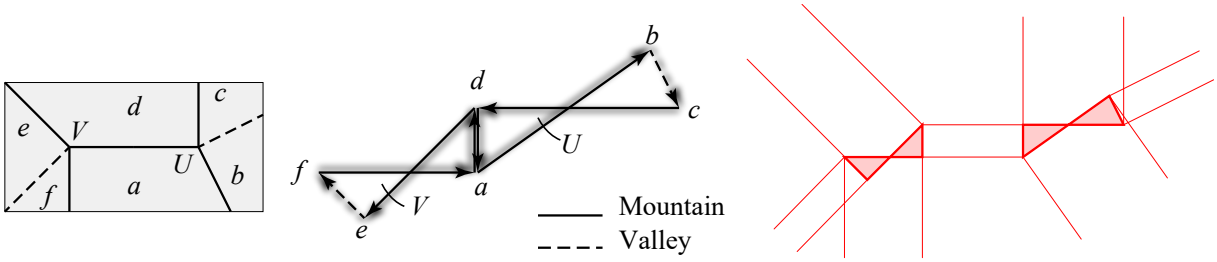

Figure 2: Left: A crease pattern of origami. Middle: A zero-area reciprocal diagram of the crease pattern. Right: We also use a cantellated diagram for visualization purpose.

in the context of folding motion was not mathematically clarified, as his interpretation of zero-area reciprocal diagram as the "infinitesimal" behavior of folding near very flat unfolded state [5] leaves some ambiguity.

Zero area reciprocal diagram is catching the researchers' attentions again after 2000s in the context of origami engineering. Watanabe and Kawaguchi [11] presented the zero-area reciprocal diagram as a method to judge rigid foldability and showed that the existence of such diagram is a necessary condition for rigid foldability but not sufficient in general. Further, Watanabe [10] shows the relation between the second-order approximation of rigid foldability and the zero-area reciprocal diagram.

In this paper, we will clarify the geometric meaning of zero-area reciprocal diagram by first verifying the equivalence of the existence of zero-area dual polygon and the second-order rigid foldability, and then by showing this second-order condition is actually sufficient condition of finite rigid foldability in the special types of patterns, namely, a single vertex pattern and a flat-foldable degree-4 multi-vertex origami. The contribution of this paper is summarized as:

1. The equivalence of zero-area reciprocal diagram and second-order rigid foldability.
2. The equivalence of the existence of zero-area reciprocal diagram and the finite rigid foldability for a single-vertex case.
3. The equivalence of the existence of zero-area reciprocal diagram and the finite rigid foldability for a flat-foldable degree-4 multi-vertex origami.
4. Analysis of design examples of rigidly or approximately foldable patterns designed by Huffman.

2. Definitions

Reciprocal Diagram A crease pattern C is a planar graph on a polygonal piece of paper P such that it partitions P into multiple faces. Consider the dual graph D of C; the dual graph is a planar graph whose faces, edges, and vertices correspond to the vertices, edges, and faces of C, respectively. The *reciprocal diagram* R of C is a mapping (with potential self-intersection) of D on to the plane with the following properties:

1. The edge i^* in R mapped from crease i in C is a straight segment perpendicular to i.
2. The *face loop* is defined for each face v^* in R corresponding to vertex v in C as the sequence of dual edges corresponding to the edges in counterclockwise order around v.
3. Each edge $i*$ of reciprocal diagram has assigned *sign* σ_i, such that along any face loop of v^*, the direction of the edge $i*$ is 90° clockwise or counterclockwise rotation of the vector along the original crease i from corresponding vertex v if sign is plus or minus, respectively.

Zero-area reciprocal diagram of C is a reciprocal diagram of C where the signed area of each face in counterclockwise orientation is zero.

We also propose the visualization of the reciprocal diagram, *cantellated diagram*, which is a potentially self-intersecting cantellation of the original diagram, whose generated dual polygon at the vertex is congruent to the corresponding face of the reciprocal diagram (Figure 2 Right.) The existence of (zero-area) cantellated diagram is equivalent to the existence of (zero-area) reciprocal diagram.

Rigid Foldability We follow an usual definitions of rigid foldability [1] but with allowing some edges not to fold at all. *Rigid folded state* of origami by crease pattern C is a piecewise isometric homeomorphism of a piece of paper P, where each face surrounded by crease of C and the boundary of P stays congruent after folded. *Fold angle* of a crease is the signed angle formed by the normals of incident faces, such that it is positive (negative) if the front side (back side) of the paper gets closer.

Each fold angle determines the relative position of adjacent faces, which in turn, determines the positions of all faces. Thus a given folded state (relative to one of the face) can be uniquely represented by a point in $\mathbb{R}^{E_{in}}$, where each axis represents the fold angle of each crease. This space is called the *parameter space*. The set of point on parameter space that represents a valid folded state is called *configuration space*, which is the solution space of piecewise isometry constraints. *Rigid foldability* is a problem of asking if there is a finite length continuous path from a point within the configuration space.

Condition of Folded State A planar piece of paper homeomorphic to a disk with specified fold angles is judged to be a valid rigid folded state if and only if there is no paper crossings and it satisfies all of the condition around each vertex: for each interior vertex with incident edges $i = 0, \ldots, n-1$ with fold angles ρ_i and direction vector $\boldsymbol{\ell}_i = (\ell_i^x, \ell_i^y, \ell_i^z)^\mathsf{T}$ ($\ell_i^z = 0$ when we are at the flat state) [6, 2],

$$\mathbf{F} := \mathbf{R}(\boldsymbol{\ell}_0, \rho_0)\mathbf{R}(\boldsymbol{\ell}_1, \rho_1) \cdots \mathbf{R}(\boldsymbol{\ell}_{n-1}, \rho_{n-1}) = \mathbf{I}_3, \tag{1}$$

where $\mathbf{R}(\boldsymbol{\ell}_i, \rho_i)$ is an orthogonal matrix representing the rotation by angle ρ_i about an axis along $\boldsymbol{\ell}_i$ passing through the origin (Figure 3 Left). In this paper, we can ignore the paper crossing because we are interested in the neighborhood of configuration space near the flat state, where no potential intersection exists.

Here, $\mathbf{R}(\boldsymbol{\ell}_i, \rho_i)$ can be described by Rodregues's formula as

$$\mathbf{R}(\boldsymbol{\ell}_i, \rho_i) = \mathbf{I}_3 + \sin\rho\,[\boldsymbol{\ell}_{i\times}] + (1 - \cos\rho)\,[\boldsymbol{\ell}_{i\times}]^2,$$

where $[\boldsymbol{\ell}_{i\times}]$ is a cross product operator which is is a skew-symmetric matrix defined such that $[\boldsymbol{\ell}_{i\times}]\,\mathbf{p} = \boldsymbol{\ell}_i \times \mathbf{p}$ for any vector $\mathbf{p}$.

$$[\boldsymbol{\ell}_{i\times}] := \begin{bmatrix} 0 & -\ell_i^z & \ell_i^y \\ \ell_i^z & 0 & -\ell_i^x \\ -\ell_i^y & \ell_i^x & 0 \end{bmatrix}.$$

n-th order rigid foldability: We say an origami crease pattern is n-th order rigidly foldable ($n = 1, 2$) if there is a parameterized C^1 path $\boldsymbol{\rho}(t)$ in the parameter space with nontrivial initial speed $\dot{\boldsymbol{\rho}}(0)$ such that $\mathbf{F}$ is at most $o(t^{n+1})$.The motion $\boldsymbol{\rho}(t)$ is called n-th order rigid folding motion. First order rigid

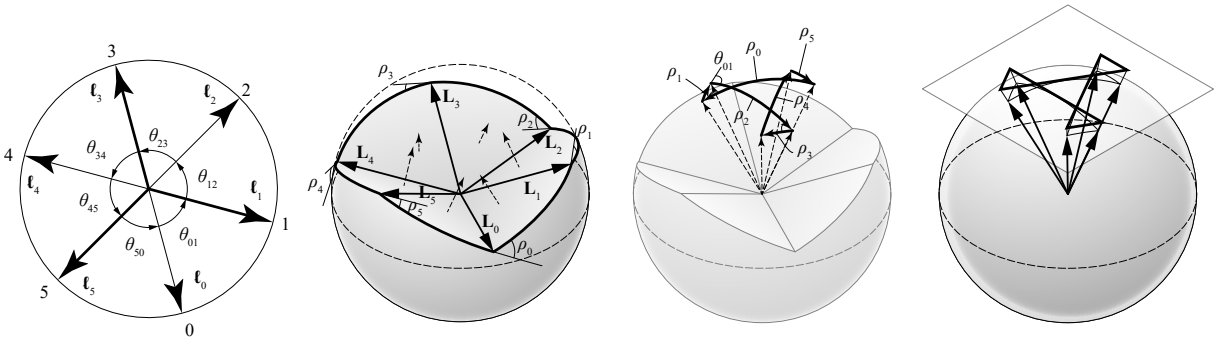

Figure 3: Single vertex rigid origami. Gauss Map and its projection to a plane.

foldability is also called *infinitesimal rigid foldability*.

Corollary 1 *n-th order rigid foldability implies $n-1$-th rigid foldability.*

3. First Order Rigid Foldability

Because $\mathbf{F}$ is C^∞, its first-order approximation can be given as

$$\mathbf{F} = \mathbf{I}_3 + \sum_{i=0}^{n-1} \left.\frac{\partial \mathbf{F}}{\partial \rho_i}\right|_{\boldsymbol{\rho}=\mathbf{0}} \dot{\rho}_i \Delta t + o(\Delta t^2), \tag{2}$$

where the partial derivative of $\mathbf{F}$ in the second term is

$$\left.\frac{\partial \mathbf{F}}{\partial \rho_i}\right|_{\boldsymbol{\rho}=\mathbf{0}} = \mathbf{R}(\boldsymbol{\ell}_0, \rho_0) \cdots \mathbf{R}(\boldsymbol{\ell}_i, \rho_i) \left[\boldsymbol{\ell}_{i\times}\right] \mathbf{R}(\boldsymbol{\ell}_{i+1}, \rho_{i+1}) \cdots \mathbf{R}(\boldsymbol{\ell}_{n-1}, \rho_{n-1})\big|_{\boldsymbol{\rho}=\mathbf{0}} = \left[\boldsymbol{\ell}_{i\times}\right]. \tag{3}$$

Here, we used that

$$\frac{\partial \mathbf{R}(\boldsymbol{\ell}_i, \rho_i)}{\partial \rho_i} = \cos\rho \left[\boldsymbol{\ell}_\times\right] + \sin\rho \left[\boldsymbol{\ell}_\times\right]^2 = \mathbf{R}(\boldsymbol{\ell}_i, \rho_i) \left[\boldsymbol{\ell}_\times\right].$$

Therefore, the necessary and sufficient condition for the first-order rigid foldability is to obtain the motion's first-order derivative $\dot{\rho}_i$ making the second term of Equation 2 zero.

$$\sum_{i=0}^{n-1} \dot{\rho}_i \left[\boldsymbol{\ell}_{i\times}\right] = \mathbf{0}. \tag{4}$$

for each vertex. Equivalently, using $\boldsymbol{\omega}_i = \dot{\rho}_i \boldsymbol{\ell}_i = (\omega_i^x, \omega_i^y, \omega_i^z)^\mathsf{T}$,

$$\sum_{i=0}^{n-1} \dot{\rho}_i \boldsymbol{\ell}_i = \sum_{i=0}^{n-1} \boldsymbol{\omega}_i = \mathbf{0}. \tag{5}$$

Theorem 2 *The existence of nontrivial reciprocal diagram of crease pattern C is the necessary and sufficient condition for the first-order rigid foldability by C.*

Proof: For sufficiency, assume that there is a nontrivial reciprocal diagram. For each edge $i*$ of reciprocal diagram, we can define signed length ℓ_{i^*}, the length of $i*$ with its sign σ_i. If we set $\dot{\rho}_i = \ell_{i^*}$, then Equation 5 represents the closure of corresponding each face loop rotated by 90° in counterclockwise

direction. For necessity, given Equations 5 for each vertex, we can draw its dual polygon for each vertex such that each edge has length of $|\rho_i|$ and signs of $\mathrm{sign}(\rho_i)$. Such dual polygon can be translated to tessellate a plane because their shared edges have compatible directions and lengths. □

An important fact from Equation 5 is that in a flat unfolded state or origami, z element of the equation degenerates to zero no matter of choice of fold speed assignment. Only two equations out of three constraints is actually active in this singular position, but once it is in a generic folded position, the third equation constrains the system. As a result, a 3-valency vertex is infinitesimally rigidly foldable although not rigidly foldable. Also, the flat state is a bifurcation point of different folding paths for a rigidly foldable system.

4. Second order Rigid Foldability

Now, let us consider the second-order rigid foldability.

$$\mathbf{F} = \mathbf{I} + \sum_{i=0,\dots,n-1} \frac{\partial \mathbf{F}}{\partial \rho_i}\dot{\rho}_i\bigg|_{\boldsymbol{\rho}=\mathbf{0}} \Delta t + \frac{1}{2}\left(\sum_{i=0}^{n-1}\sum_{j=0}^{n-1} \frac{\partial^2 \mathbf{F}}{\partial \rho_i \partial \rho_j}\dot{\rho}_i\dot{\rho}_j + \sum_{i=0}^{n-1} \frac{\partial \mathbf{F}}{\partial \rho_i}\ddot{\rho}_i\right)\bigg|_{\boldsymbol{\rho}=\mathbf{0}} \Delta t^2 + o(\Delta t^3) \quad (6)$$

Here, the second-order derivative of the total rotation is

$$\frac{\partial^2 \mathbf{F}}{\partial \rho_i \partial \rho_j} = \mathbf{R}(\boldsymbol{\ell}_0, \rho_0)\cdots\mathbf{R}(\boldsymbol{\ell}_i, \rho_i)\left[\boldsymbol{\ell}_{i\times}\right]\cdots\mathbf{R}(\boldsymbol{\ell}_j, \rho_j)\left[\boldsymbol{\ell}_{j\times}\right]\cdots\mathbf{R}(\boldsymbol{\ell}_{n-1}, \rho_{n-1}), \quad (7)$$

when $i \le j$. This has the value at the flat state of

$$\mathbf{H}_{i,j} := \frac{\partial^2 \mathbf{F}}{\partial \rho_i \partial \rho_j}\bigg|_{\boldsymbol{\rho}=\mathbf{0}} = \begin{cases} \left[\boldsymbol{\ell}_{i\times}\right]\left[\boldsymbol{\ell}_{j\times}\right] & i \le j \\ \left[\boldsymbol{\ell}_{j\times}\right]\left[\boldsymbol{\ell}_{i\times}\right] & i > j \end{cases} \quad (8)$$

The former $i \le j$ case is calculated as

$$\left[\boldsymbol{\ell}_{i\times}\right]\left[\boldsymbol{\ell}_{j\times}\right] = \begin{bmatrix} -\ell_i{}^y\ell_j{}^y & \ell_i{}^y\ell_j{}^x & 0 \\ \ell_i{}^x\ell_j{}^y & -\ell_i{}^x\ell_j{}^x & 0 \\ 0 & 0 & -\ell_i{}^x\ell_j{}^x - \ell_i{}^y\ell_j{}^y \end{bmatrix} \quad (9)$$

We can easily check that the latter case is the transpose of the former case. A first-order rigid folding motion $\boldsymbol{\rho}$ is a second-order rigid folding motion if and only if $\dot{\boldsymbol{\rho}}$ and $\ddot{\boldsymbol{\rho}}$ can be given such that the third term of Equation 6 vanishes.

$$\sum_{i,j}\mathbf{H}_{i,j}\dot{\rho}_i\dot{\rho}_j + \sum_i \left[\boldsymbol{\ell}_{i\times}\right]\ddot{\rho}_i =$$

$$\sum_{i,j}\begin{bmatrix} -\ell_i{}^y\ell_j{}^y & \ell_a{}^y\ell_b{}^x & 0 \\ \ell_a{}^x\ell_b{}^y & -\ell_i{}^x\ell_j{}^x & 0 \\ 0 & 0 & -\ell_i{}^x\ell_j{}^x - \ell_i{}^y\ell_j{}^y \end{bmatrix}\dot{\rho}_i\dot{\rho}_j + \sum_i \begin{bmatrix} 0 & 0 & \ell_i^y \\ 0 & 0 & -\ell_i^x \\ -\ell_i^y & \ell_i^x & 0 \end{bmatrix}\ddot{\rho}_i \qquad = \mathbf{0}$$

where $a = \min(i,j)$ and $b = \max(i,j)$. Notice the perpendicularity of first and second term, which means that they must be both $\mathbf{0}$. The second term can be set to zero by either a trivial acceleration,so we only need to care about the first term.

The diagonal elements of the first term $\sum \mathbf{H}_{i,j}\dot{\rho}_i\dot{\rho}_j$ are all zero because of Equation 5. For example, $\sum_{i,j}\ell_i^x\ell_j^x\dot{\rho}_i\dot{\rho}_j = (\sum_i \omega_i^x)(\sum_j \omega_j^x) = 0$. So, we look at the remaining elements $(1,2)$ and $(2,1)$ of the matrix, and consider their summation and difference. The summation again is zero because of

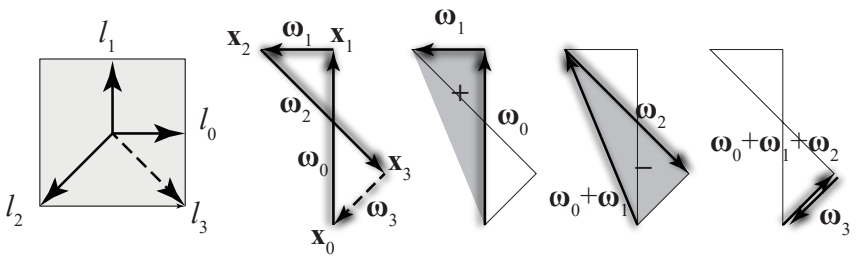

Figure 4: The signed area of a reciprocal face.

Equation 5.

$$\sum_{i,j}(\mathbf{H}_{i,j}(2,1)\ell + \mathbf{H}_{i,j}(1,2))\dot{\rho}_i\dot{\rho}_j = \sum_{i,j}(\omega_i^x\omega_j^y + \omega_i^y\omega_j^x) = 0$$

Their difference is

$$\sum_{i,j}(\mathbf{H}_{i,j}(2,1)\ell - \mathbf{H}_{i,j}(1,2))\dot{\rho}_i\dot{\rho}_j. = 2\sum_{i,j(i<j)}\|\boldsymbol{\omega}_i \times \boldsymbol{\omega}_j\|$$

Therefore, $\boldsymbol{\rho}$ is second-order rigidly foldable motion if and only if it satisfies Equation 5 and

$$\sum_{i,j(i<j)}\|\boldsymbol{\omega}_i \times \boldsymbol{\omega}_j\| = 0 \tag{10}$$

Theorem 3 *A crease pattern is second-order rigidly foldable if and only if there exists a non-trivial zero-area reciprocal diagram.*

Proof: For necessity, assume that Equations 5 and 10 are satisfied. Because of Equation 5, there exits a reciprocal diagram, and we let the position of the node of reciprocal diagram as $\mathbf{x}_i$ such that $\boldsymbol{\omega}_i = \mathbf{x}_{i+1} - \mathbf{x}_i$ for each vertex. Now, Equation 10 can be written as

$$\begin{aligned}\sum_{i,j(i<j)}\|\boldsymbol{\omega}_i \times \boldsymbol{\omega}_j\| \\ = \|(\boldsymbol{\omega}_0 + \cdots + \boldsymbol{\omega}_{n-2}) \times \boldsymbol{\omega}_{n-1}\| + \|(\boldsymbol{\omega}_0 + \cdots + \boldsymbol{\omega}_{n-3}) \times \boldsymbol{\omega}_{n-2})\| + \cdots + \|\boldsymbol{\omega}_0 \times \boldsymbol{\omega}_1\| \\ = \sum_{i=1}^{n-1}\|(\mathbf{x}_i - \mathbf{x}_0) \times (\mathbf{x}_{i+1} - \mathbf{x}_i)\|\end{aligned}$$

Since $\|(\mathbf{x}_i - \mathbf{x}_0) \times (\mathbf{x}_{i+1} - \mathbf{x}_i)\|$ represents 2 times the signed area of triangle formed by $\mathbf{x}_0, \mathbf{x}_i, \mathbf{x}_{i+1}$, their summation is the signed area of the polygon $\mathbf{x}_0, \mathbf{x}_1, \ldots, \mathbf{x}_{n-1}$. Therefore, each face of the reciprocal diagram has zero-area. Figure 4 shows an example of degree-4 vertex. On the other hand, if the reciprocal diagram is zero-area, it satisfies Equation 10, so it is also sufficient. □

5. Single Vertex Rigid Foldability

In general, second-order rigid foldability does not imply finite rigid foldability. However, second-order rigid foldability is a sufficient judge of finite rigid foldability for a single-vertex origami.

Theorem 4 *A single-vertex origami is rigidly foldable if and only if it has a nontrivial zero-area dual.*

Proof: Necessity is obvious as rigid foldability implies second-order rigid foldability. For sufficiency, assume that a zero-area reciprocal diagram exists. Consider adding a slit along one of the creases and folding the other creases proportionally to the folding speed given by the reciprocal digram. This structure can be illustrated as a spherical linkage by taking the intersection of the surrounding faces with a small sphere centering the vertex. We claim that the gap at the slit can be glued back together by a mall modification of fold angles; more specific proof follows.

First, we can safely assume that there are at least four creases with nontrivial speeds. (This is because a nontrivial reciprocal polygon has at least two non-trivial edges. If there are only two of such creases, they must be collinear, and the proportional folding is exactly a valid rigid folding as desired. If there are only three of such creases, the reciprocal diagram forms a triangle, whose area cannot be zero.) Now, take three consecutive creases i, j, and k, such that the summation of angles θ_{ij} between ij and θ_{jk} between jk is smaller than 180° (Figure 5). Now, assume that the slit separates crease k into two k and k' (such that k side is connected), and fold the rest of the angles according to the reciprocal diagram. We assume that the fold angle at j equals some time parameter t. The distance $\theta_{ik'}$ between i and k' is approximated by θ_{ik} in second order. This is calculated using spherical lows of cosines as follows.

$$\cos(\theta_{ik'} + o(t^3)) = \cos(\theta_{ik}) = \cos\theta_{ij}\cos\theta_{jk} + \sin\theta_{ij}\sin\theta jk\cos(\pi - t).$$

By the Taylor expansion of cosines and sines, we get

$$\cos\theta_{ik'} - \cos(\theta_{ij} + \theta_{jk}) = \frac{t^2}{2}\sin\theta_{ij}\sin\theta_{jk} + o(t^3) > 0 \tag{11}$$

Therefore, $\theta_{ik'} < \theta_{ij} + \theta_{jk}$ holds for the range of sufficiently small t, and thus the gap is connected. □

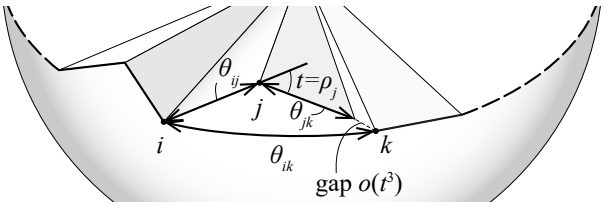

Figure 5: Using two flaps to fill the gap of $o(t^3)$.

6. Multiple Vertex Cases

For a pattern with multiple vertices, zero-area reciprocal diagram does not imply rigid foldabilty in general. The third author designed series of origami crease patterns, which apparently are based on zero-area reciprocal diagram. Here, we show a family of patterns that are rigidly foldable and a family that are only approximately rigid foldable.

Exactly Rigidly Foldable: Flat foldable Degree-4 Pattern A pattern made only with flat-foldable degree-4 vertex has a property that if there exits a rigid folding, then the folding angles measured by tangent of half angles $\tan\frac{\rho}{2}$ are proportional to each other [4, 5, 9]. A series of patterns designed by Huffman falls into this category. Figure 6 shows one of such patterns with zero-area reciprocal diagram, which are all rigidly foldable. In fact, we can show that any origami pattern in this category is rigidly foldable.

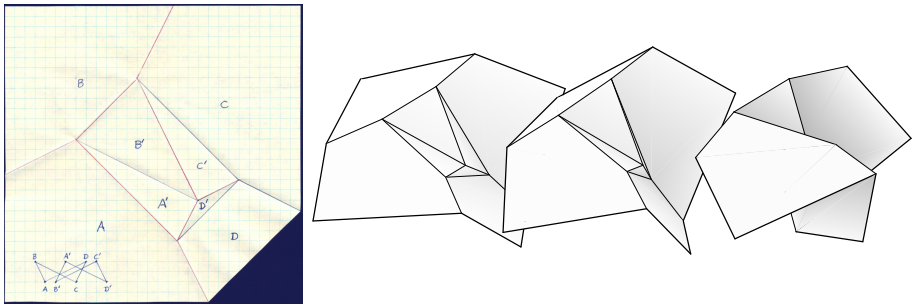

Figure 6: A pattern formed by Flat-foldable degree-4 vertices. Left: Huffman's sketch with reciprocal diagram. Right: Folding simulation by *Freeform Origami*.

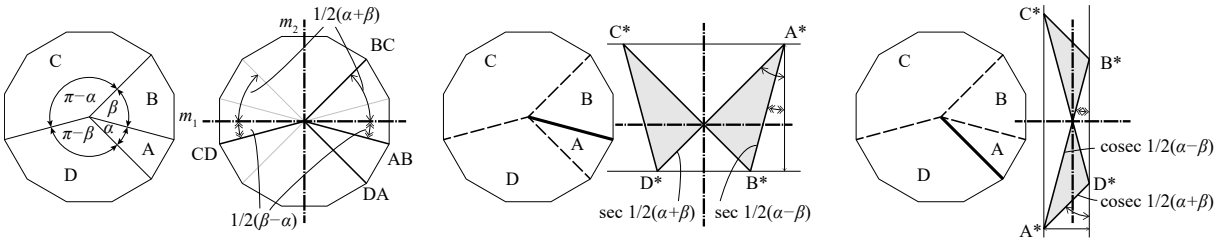

Figure 7: Zero-area reciprocal diagram of flat-foldable degree-4 vertex.

Theorem 5 *An origami crease pattern that is composed only of degree-4 vertices with supplementary opposite angles is rigidly foldable if and only if there exists a nontrivial zero-area reciprocal diagram.*

Proof: Assume there is a zero-area reciprocal diagram. Consider a vertex with faces A, B, C, D with sector angles $\alpha, \beta, \pi-\alpha, \pi-\beta$, respectively. (1) Because of this supplementary angle property, when each crease is drawn as a full line, there exists a pair of perpendicular axes m_1 and m_2 that mirror reflects creases AB to CD and BC to DA. (2) Also, because reciprocal quadrangle $A^*B^*C^*D^*$ is zero-area, the line A^*C^* is parallel to B^*D^* (Figure 7). From properties (1) and (2), the possible reciprocal quadrangles are constrained to have A^*C^* parallel or perpendicular to the m_1 and m_2. This reduces to two cases as shown in Figure 7.

$$(\omega_{AB}, \omega_{BC}, \omega_{CD}, \omega_{DA}) = \begin{cases} \left(-\cos\frac{\alpha+\beta}{2}, \cos\frac{\alpha-\beta}{2}, \cos\frac{\alpha+\beta}{2}, \cos\frac{\alpha-\beta}{2}\right) \\ \left(\sin\frac{\alpha+\beta}{2}, -\sin\frac{\alpha-\beta}{2}, \sin\frac{\alpha+\beta}{2}, \sin\frac{\alpha-\beta}{2}\right) \end{cases}$$

It can be checked that the path

$$\left(\tan\frac{\rho_{AB}}{2}, \tan\frac{\rho_{BC}}{2}, \tan\frac{\rho_{CD}}{2}, \tan\frac{\rho_{DA}}{2}\right) = (\omega_{AB}, \omega_{BC}, \omega_{CD}, \omega_{DA})$$

satisfies Equation 1, and thus is a continuous rigid folding path. Zero-area polygons are compatible in the reciprocal diagram, so the existence of zero-area reciprocal diagram imply the existence of rigid folding motion. □

Approximately Rigidly Foldable: Spiral Pattern General assembly of zero-area polygons does not lead to a finite mechanism. Figure 8 shows examples of spiral origami designed by the third author based on reciprocal diagrams. Figure 9 shows the reconstructed cantellation diagram. To verify, we performed a folding simulation using *Freeform Origami* [8] (Figure 8 Bottom). We observed a small flex with some numerical error and significantly slow convergence to the flat state. The slow convergence seemingly

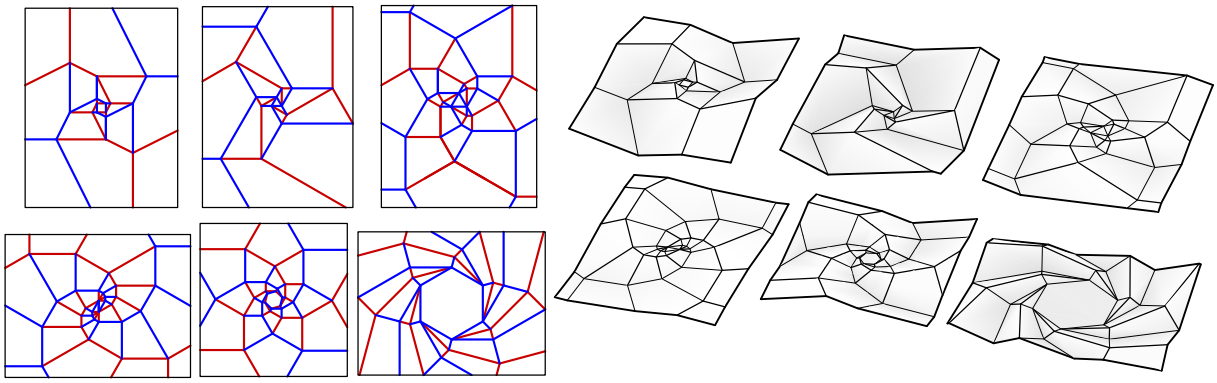

Figure 8: Series of spiral designs that has zero-area reciprocal diagram. They are only approximately rigidly foldable.

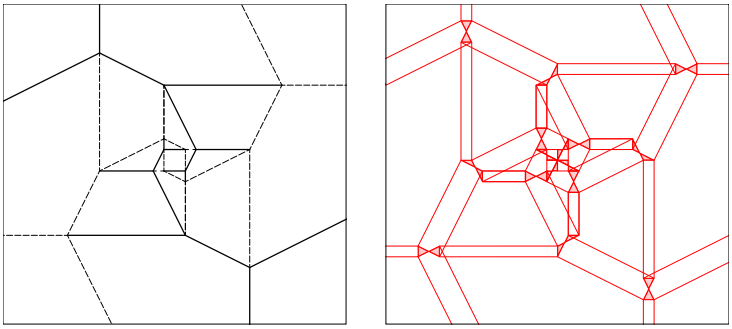

Figure 9: Left: One of patterns from Figure 8. Right: Cantellated visualization of zero-area reciprocal diagram.

originates from the failure in the Newton-Raphson method when dealing with non-quadratic errors along the second-order rigidly foldable path.

7. Conclusion

We showed the equivalence of zero-area reciprocal diagram and the second-order rigid foldability for origami crease pattern. Single vertex origami and an origami pattern with flat foldable degree-4 vertices are special cases where the second-order rigid foldability leads to finite rigid foldability. Compared to the characterization of rigid foldability of a single-vertex [1] or origami with flat-foldable degree-4 vertices [9], the proposed graphical method has an advantage that we can construct the folding speed as the signed length of the diagram. We expect that the zero-area reciprocal diagram in the form of cantellated diagram can be applied as a good graphical tool for the design of rigidly foldable mechanisms, especially when the folding speed needs to be controlled. As an example, Figure 10 shows a rigidly foldable mechanism with rapidly amplifying folding speeds. This continuous one-DOF mechanism mimics a sequential folding process. We also showed variational designs of second-order rigidly foldable but not rigidly foldable patterns. As such patterns can approximate a rigid folding mechanism, we suspect that these patterns have many potential engineering applications for deformable and deployable structures.

Acknowledgment

This work was discussed at the 2016 Bellairs Workshop on Computational Geometry, co-organized by Erik Demaine and Godfried Toussaint. We thank the other participants of the workshop for stimulating

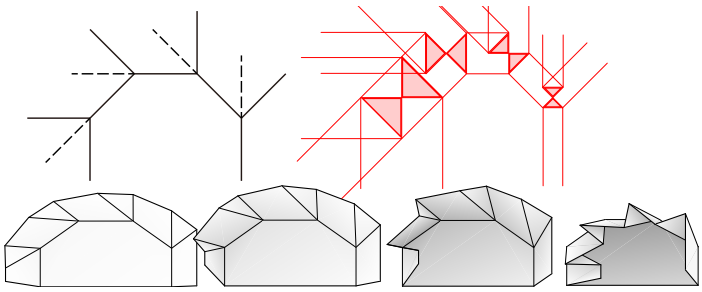

Figure 10: A "sequential" rigid folding produced by amplifying folding speeds.

discussions. We thank the Huffman family for access to the third author's work, and permission to continue in his name.

References

[1] Abel, Z., Cantarella, J., Demaine, E. D., Eppstein, D., Hull, T. C., Ku, J. S. , Lang, R. J. and Tachi, T. Rigid origami vertices: Conditions and forcing sets. *Journal of Computational Geometry*, 7(1), 2016.

[2] belcastro, s.-m. and Hull, T. A mathematical model for non-flat origami. In *Origami3: Proceedings of the 3rd International Meeting of Origami Mathematics, Science, and Education*, pages 39–51, 2002.

[3] Cremona, L. *Graphical Statics (English translation)*. Oxford University Press, 1890.

[4] Huffman, D. Curvature and creases: a primer on paper. *IEEE Transactions on Computers*, C-25(10):1010–1019, 1976.

[5] Huffman, D. A. Surface curvature and applications of the dual representation. *Workshop on Computer Vision Systems*, pages 213–222, 1977.

[6] Kawasaki, T. $R(\gamma) = \mathbf{I}$. In *Proceedings of the Second International Meeting of Origami Science and Scientific Origami*, pages 31–40, 1997.

[7] Maxwell, J. C. *On Reciprocal Diagrams in Space and their relation to Airy's Function of Stress*. 1890.

[8] Tachi, T. Freeform origami. `http://www.tsg.ne.jp/TT/software#ffo`.

[9] Tachi, T. Generalization of rigid-foldable quadrilateral-mesh origami. *Journal of the International Association for Shell and Spatial Structures*, 50(3):173–179, December 2009.

[10] Watanabe, N. (in Japanese) extraction of foldable mode in a singular state of panel-hinge model. In *Proceedings of 31th Symposium on Aerospace Structure and Materials ,JAXA/ISAS*, number A6000047014, 2015.

[11] Watanabe, N. and Kawaguchi, K. The method for judging rigid foldability. In R. Lang, editor, *Origami^4: The Fourth International Conference on Origami in Science, Mathematics, and Education*, pages 165–174. A K Peters, 2009.

[12] Whiteley, W. Motions and stresses of projected polyhedra. *Structural Topology*, 7:13–38, 1982.